Original Article

ISSN: 1735-0344 *Tanaffos 2021; 20(4): 353-362*

TANAFFOS

A Lysine-Functionalized Graphene Oxide-Based Nanoplatform for Delivery of Fluorouracil to A549 Human Lung Cancer Cells: A Comparative Study

Maryam Ashjaran [1], Mirzaagha Babazadeh[1], Abolfazl Akbarzadeh [2,3], Soodabeh Davaran[4], Roya Salehi [4]

[1] Department of Chemistry, Tabriz Branch, Islamic Azad University, Tabriz, Iran, [2] Drug Applied Research Center, Tabriz University of Medical Sciences, Tabriz, Iran, [3] Universal Scientific Education and Research Network (USERN), Tabriz, Iran, [4] Department of Medical Nanotechnology, Faculty of Advanced Medical Sciences, Tabriz University of Medical Sciences, Tabriz, Iran.

Received: 2 October 2020
Accepted: 11 February 2021

Correspondence to: Babazadeh M
Address: Department of Chemistry, Tabriz Branch, Islamic Azad University, Tabriz, Iran
Email address: babazadeh@iaut.ac.ir

Background: Today, increasing attention is being paid to the application of biocompatible polymers as drug carriers with low cytotoxicity in drug delivery systems to enhance the therapeutic effects of anticancer agents.

Materials and Methods: In this study, a biocompatible synthetic polymer (grafted on graphene oxide), composed of N-isopropylacrylamide and 1-vinyl-2-pyrrolidone with L-lysine segments (Lys/PNIPAM-PVP/GO), was developed as a nano-vehicle for the drug. This platform was used for the delivery of fluorouracil (FU) to A549 human lung cancer cells. The superior characteristics of the platform included low-cost precursors, easy synthesis, and the presence of many functional groups for loading drugs. To determine and compare the cytotoxic effects of free FU and its formulated form on the A549 cells, MTT assay was performed; the results showed no significant toxicity difference between the two treated groups (free and formulated FU).

For further evaluations, cellular uptake assays were performed via fluorescence microscopy and flow cytometry.

Results: Both analyses revealed the low internalization of nano-vehicle into the A549 cells, with 4.31% and 8.75% cellular uptakes in the first two and four hours of treatment. Therefore, the low penetration rate reduced the toxicity of drug-loaded nano-vehicle.

Conclusion: Finally, DAPI staining and Annexin V-FITC staining were performed as complementary techniques to determine cell apoptosis.

Key words: Graphene oxide; Drug carrier; Fluorouracil; A549 cell line; Lung cancer

INTRODUCTION

Cancer refers to an abnormal and uncontrollable division of cells (1). Many types of cancer have been identified so far, including breast cancer, colorectal cancer, prostate cancer, skin cancer, stomach cancer, and lung cancer (2-4). Among these cancers, lung cancer is the most common cause of cancer-related death. According to the World Health Organization (WHO) statistics, cancer is a leading cause of mortality worldwide, accounting for 9.6 million deaths in 2018. Meanwhile, lung cancer is responsible for 2.1 million deaths (5, 6).

A surgery can be the most successful when a tumor has not spread to other organs. However, surgery is not the most straightforward approach for the treatment of many cancers. Therefore, chemotherapy is used as an essential tool with combination therapy in various types of cancer treatment (7, 8). Nevertheless, chemotherapeutic agents have many toxic side effects, such as anemia, nausea,

infection, and neutropenia (9, 10). Accordingly, researchers in both nanotechnology and nanomaterial sciences have attempted to reduce these side effects by designing and fabricating nano-sized drug carriers (11-15).

Researchers are particularly interested in using drug carriers as vehicles in drug delivery systems and other biomedical applications (16, 17). Many platforms have been developed and investigated as carriers, such as liposomes, micelles, nanocomposites, magnetic nanoparticles, silica nanoparticles, and carbon-based nanostructures (18-24). All of these platforms have advantages and disadvantages. However, carbon-based materials, such as graphene and carbon nanotubes, have many benefits in drug delivery systems due to high-density active sites and ultrahigh surface areas for loading drugs. However, they are highly hydrophobic due to the absence of oxygen-containing hydrophilic groups.

Graphene oxide (GO) is composed of oxygen-containing hydrophilic groups on its surface. The GO platform aggregates under physiological conditions (23, 25). Aggregation is a negative feature for materials in biomedical applications; therefore, modification of graphene and GO is necessary. Generally, GO is a carbon-based platform. Both sides of its single-atom layer sheet have the capacity for surface modifications (25-27). To improve GO deficiencies, surface modifications have been made using natural and synthetic polymers (28, 29). Polymers with thermal and pH-responsive properties, without toxic effects, are proper candidates in drug delivery system applications due to their role in the microenvironment conditions and biocompatibility (30, 31).

Common synthetic polymers for modification of GO include polyethylene glycol (PEG), poly(N-isopropylacrylamide) (PNIPAM), polycaprolactone (PCL), polylactic acid (PLA), poly-D,L-lactide-co-glycolide (PLGA), and polyvinylpyrrolidone (PVP). PVP is a synthetic, non-ionic, non-toxic, and biocompatible polymer. The biocompatible nature of PVP makes it suitable for tissue engineering and drug delivery systems. The hydrophilic nature of PVP can be successfully used to deliver hydrophobic drugs (32). Also, thermo-responsive polymers with a lower critical solution temperature (LCST) have been investigated for various biomedical and pharmaceutical formulations. PNIPAM is a thermosensitive polymer, used in many drug delivery systems, including cancer therapeutics (33). Various graphene-based platforms have been developed so far for biomedical applications (34). Researchers, including the authors of this study, have utilized functionalized nanoscale GO as nanocarriers for drug and gene delivery systems (35-37).

In this study, a biocompatible poly(N-isopropylacrylamide-co-vinylpyrrolidone) (PNIPAM-PVP) platform was synthesized and grafted on the surface of GO nanosheets, according to our previous research (38). Lysine, as an amino acid with both amine and carboxylic acid functional groups, attaches to the surface of GO to increase the grafting functional groups and bioavailability. The antitumor efficacy of fluorouracil (FU)-loaded nano-platform and FU-free nano-platform was assesed in the A549 human lung cancer cells by MTT cytotoxicity assay, cellular uptake assays, DAPI staining, and apoptosis assays (FITC-Annexin V staining)..

MATERIALS AND METHODS

Materials

Some reagents were used for the preparation of GO, including graphite, sodium nitrate ($NaNO_3$), concentrated sulfuric acid (H_2SO_4, 95-98%), hydrochloric acid (HCl, 37%), potassium permanganate ($KMNO_4$), and hydrogen peroxide (H_2O_2, 30%), purchased from Merck Co. (USA). For the polymerization reaction, two monomers, including N-isopropylacrylamide (NIPAM; 97%) and 1-vinyl-2-pyrrolidinone (VP; 95%) were obtained from Sigma-Aldrich Co. (USA). Two other regents, that is, 2,2'-azobis(2-methylpropionitrile) (AIBN) and lysine hydrochloride (Lys; 98%), were also provided by Merck Co. (USA).

All solvents were purified according to standard purification methods. FU, as an anticancer drug, was

purchased from Sigma Aldrich Co. (USA). All materials used in the biological processes and assays, including 3-(4,5-dimethylthiazol-2-yl)-2,5-diphe-nyltetrazolium bromide (MTT), trypsin, fetal bovine serum (FBS), and RPMI medium, were purchased from Gibco BRL Life Technologies (USA). The eBioscience™ Annexin V-FITC Apoptosis Detection Kit was also purchased from Invitrogen Co. (USA). Finally, the A549 cells, as human lung cancer cells, were provided by the Cell Bank of Pasteur Institute of Iran (Tehran, Iran).

Preparation of graphene-based nano-vehicles

PNIPAM-PVP-grafted GO (PNIPAM-PVP/GO) was synthesized as a nano-vehicle, according to our previous study (13). For the synthesis of GO as a platform, a graphite-based nano-vehicle was fabricated, based on the modified Hummer's method with slight modifications (39). The GO-based nano-vehicle was synthesized in a reactor, equipped with a mechanical stirrer. NIPAM (3.0 g) and VP (1.0 mL) were dissolved in dimethylformamide (DMF, 40 mL) and stirred for 20 minutes. Subsequently, GO (0.7 g) was added and sonicated for an additional 20 minutes. Next, AIBN (12 mg/1 mL DMF) as a polymerization catalyst was added to the reaction and stirred vigorously.

The polymerization reaction was initiated at 70°C in a nitrogen atmosphere for 48 hours. After the reaction was completed, the reaction mixture was centrifuged and washed several times with methanol to remove unreacted reagents (NIPAM and VP monomers), and PNIPAM-PVP-grafted GO was prepared (PNIPAM-PVP/GO). For grafting lysine on the prepared platform, lysine (1.5 g) was dispersed in deionized water (20 mL) and stirred at room temperature for 24 hours to obtain lysine-functionalized graphene (Lys/PNIPAM-PVP/GO) as a nano-vehicle. At the end of the reaction process, the resulting product was freeze-dried and used in the drug loading step and other *in vitro* evaluations.

In vitro FU loading

Drug loading studies were carried out according to a previous report (21). FU was loaded on the developed nano-vehicle by incubating FU in an aqueous suspension of Lys/PNIPAM-PVP/GO (nano-vehicle). First, a nano-vehicle suspension in PBS (100 mg/5 mL; pH=7.4) was prepared at 37°C, and then, 10 mg of FU was added as an anticancer agent to the suspension and mixed by vortexing. The resulting drug/nano-vehicle suspension was incubated at 37°C in the dark for 24 hours. After incubation, the free drug was removed by centrifugation, and the produced FU/nano-vehicle was vacuum-dried and used in the release study; to increase stability, the FU/nano-vehicle powder was stored at 4°C for further analysis. The drug encapsulation efficiency (DEE) and drug loading efficiency (DLE) were calculated by a UV-Vis spectrophotometer at 264 nm, according to the following equations:

$$DEE\ (\%) = \frac{Mass\ of\ FU\ in\ nano - Vehicle\ (mg)}{Mass\ of\ free\ FU\ (mg)} \times 100 \qquad (1)$$

$$DLE(\%) = \frac{Mass\ of\ FU\ in\ nano - Vehicle\ (mg)}{Mass\ of\ nano - Vehicle\ (mg)} \times 100 \qquad (2)$$

A549 cell culture

The A549 human lung cancer cells were seeded in RPMI culture media, containing 10% FBS, 100 units/mL of penicillin, and 100 µg/mL of streptomycin, and incubated under humidified conditions in a 5% CO_2 atmosphere for 24 hours to attach to the bottom of T-flask. The cell population was monitored every day under microscope. After observing 90% of cell confluence, the cells were trypsinized and collected (40).

Cytotoxicity assay

Cytotoxicity was assessed in the A549 cells after treatment with a blank nano-vehicle, FU-free nano-vehicle, and FU-loaded nano-vehicle, as described in previous reports (7, 41). In brief, the A549 cells were seeded in 96-well plates at a density of 10^4 cells per well and incubated at 37°C in 5% CO_2 for 24 hours. The cells were attached to the bottom of the wells to grow. Meanwhile, all culture

media were replaced with fresh media, containing different concentrations of FU-free, FU-loaded, and blank nano-vehicles; the cells with no treatment were considered as the control. All procedures were performed in triplicate. After treatment for 48 hours, the culture media were withdrawn, and 180 µL of fresh medium and 20 µL of MTT solution in PBS (5 mg/mL) were added to each well and incubated for four hours. Then, the media were removed, and 100 µL of DMSO was added to dissolve the formed formazan crystals in the cells. The absorbance of solubilized formazan was detected at 570 nm, with a reference wavelength of 630 nm, using an ELISA plate reader (State Fax, 2100, Awareness Technology Inc., Palm City, FL, USA). The half maximal inhibitory concentration (IC_{50}) of each treatment was also calculated.

Cellular uptake assay

Flow cytometry and fluorescence microscopy were used to evaluate the qualitative and quantitative cellular uptakes of nano-vehicles by the A549 cells, respectively. First, the nano-vehicle was labeled with rhodamine as a fluorescent agent. For this purpose, 200 µL of rhodamine solution in DMSO (2 mg/mL) was added to 1 mL of nano-vehicle suspension (10 mg/mL of PBS, pH=7.4) via vigorous stirring in the dark overnight. Next, the rhodamine-labeled nano-vehicle was separated by centrifugation at 5000 rpm for ten minutes and washed several times with PBS solution to remove the unbound rhodamine.

For flow cytometry, the cells were seeded in six-well plates at a density of 5×10^5 per well and incubated for 24 hours to attach to the bottom of the wells. The cells treated with rhodamine-labeled nano-vehicle or without treatment were considered as the negative controls. After treatment for two and four hours, the cells were trypsinized, collected, washed with PBS (pH=7.4), and finally analyzed by flow cytometry using a FACSCalibur flow cytometer (Becton Dickinson Immunocytometry Systems, San Jose, CA, USA).

To confirm the cellular uptake of rhodamine-labeled nano-vehicle, fluorescence microscopy was used to observe the quantitative uptake. Briefly, the cells were seeded in a slide chamber at a density of 2×10^4 per chamber and incubated for 24 hours. After treatment and incubation for two and four hours, respectively, the cells were washed and fixed with formaldehyde (4% w/v). A coverslip was placed onto the glass microscope slide, and the nano-vehicle uptake was observed under a fluorescence microscope (BH2-RFCA, Olympus, Japan) (42).

DAPI staining

DAPI staining was performed to evaluate the condensed and fragmented nuclei of cancer and normal cells inducing apoptosis. Briefly, the cells were seeded in a slide chamber (2×10^4 per chamber) and incubated at 37°C to attach and grow at the bottom of each chamber. Next, a fresh culture growth medium, containing FU-free, FU-loaded, and blank nano-vehicles at $IC_{50,}$ was added. After 48 hours of treatment, the cells were washed with PBS (pH=7.4) to eliminate the treated samples. Consequently, fixation of the cells was performed with 4% wt paraformaldehyde for ten minutes at room temperature. Next, the cells were washed three times with PBS and permeabilized by Triton X-100 (0.1% w/v) for five minutes. The cells were then washed with PBS and stained with 500 ng/mL of DAPI solution for 15 minutes. DNA condensation and fragmentation of apoptotic cells were estimated with a fluorescence microscope (BH2-RFCA, Olympus, Japan). All tests were performed in triplicate (43).

Apoptosis assay

To evaluate cell apoptosis, first, the cells were seeded in six-well plates at a concentration of 5.0×10^5 cells per well in the culture medium. After 24 hours, the cell culture media were replaced with a fresh culture growth medium, containing FU-free, FU-loaded, and blank nano-vehicles at IC_{50} for 48 hours. Next, the cells were trypsinized, collected, and washed several times with cold PBS to eliminate all trypsin. The detached cells (1×10^6) were suspended in 1 mL of Annexin binding buffer. An eBioscience Annexin V-FITC Apoptosis Detection Kit was

used to stain apoptotic cells, according to the manufacturer's protocol. For this purpose, 100 µL of cell suspension, 5 µL of FITC-Annexin V, and 5 µL of propidium iodide (PI) were mixed. The cells were incubated for 15 minutes, and then, 200 µL of binding buffer was added to each suspension. Finally, the FACSCalibur flow cytometer was used for evaluating apoptotic cells (44).

Statistical analysis

All data were reported as mean±SD of three replicates. ANOVA or student's t-test was used for statistical analysis. P-values less than 0.05 were considered significant.

RESULTS

Preparation of Lys/PNIPAM-PVP/GO as a drug nano-vehicle

GO was functionalized with lysine and PNIPAM-PVP/GO via simple radical polymerization to enhance the functional groups on the GO nano-sheets (Figure 1). Due to the presence of several functional groups with a large surface area on the GO sheets, adequate space was provided for drug loading. This modified platform contained many functional groups, including hydroxyl (-OH), carboxylic acid (-COOH), amide (CO-NH-), and amine functional (-NH_2) groups, which could improve the loading efficacy of drugs. The resulting hybrid, called Lys/PNIPAM-PVP/GO, was used as a nano-vehicle for the delivery of FU to the A549 cancer cells.

Drug release profile under physiological conditions in the cancer tissue

One of the critical parameters in the design of a drug carrier is the presence of several functional groups on the surface to interact with the loaded drug. Since a high rate of drug loading increases the efficacy of therapeutics on cancer cells, the developed nano-vehicle in this study had several active sites for loading FU as an anticancer agent. FU could be loaded directly on the nano-vehicle via hydrogen bonding, electrostatic interactions, and physical interactions. Some of the drug was loaded on Lys/PNIPAM-PVP/GO via hydrogen bonding or electrostatic physical interactions with polar groups in both structures. Besides, some of the drug was loaded via π-π interactions between C-C conjugated double bonds on the GO platform and C=C bonds in the drug structure.

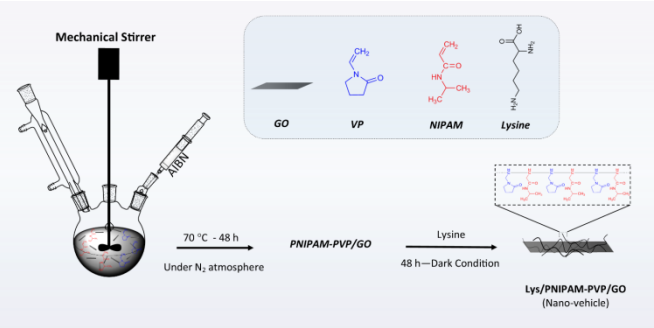

Figure 1. Preparation Lys/PNIPAM-PVP/GO (nano-vehicle) by the polymerization reaction of NIPAAM and VP in the presence of AIBN as a catalyst and functionalization with lysine

Cytotoxicity evaluation by MTT assay

The cytotoxic effects of FU-free, FU-loaded, and blank nano-vehicles on the A549 cells were assessed by the colorimetric MTT assay. To show the biocompatibility of the developed nano-vehicle, various concentrations of samples were prepared and exposed to A549 cancer cells. In our previous study, the MCF7 cells treated under the same conditions had a lower IC_{50} (about 1 µg/mL) (35). The results showed that the viability of cells in both groups decreased in a dose-dependent manner (below IC_{50} in both groups). In the current study, no cytotoxicity was observed for the blank nano-vehicle at all treated concentrations, which is comparable to the control group ($P<0.219$ for the highest dose; data not shown), suggesting that our nano-vehicle is useful for biomedical applications.

In the next step, both drugs in free and formulated forms were exposed to the A549 cells to compare the cytotoxic effects. As shown in Figure 2, there was no significant difference between FU and FU-nano vehicle in any of the groups treated with 20 µg/mL ($P<0.676$), 30 µg/mL ($P<0.413$), and 40 µg/mL ($P<0.154$), except for 10 µg/mL ($P<0.0324$) and 50 µg/mL ($P<0.015$) concentrations. Via treatment with a concentration of 10 µg/mL (much lower than IC_{50}), the cytotoxicity of FU-loaded nano-vehicle was higher than the FU-free nano-vehicle; this might be due to the delivery of FU into the cells, while at a

concentration of 50 µg/mL (above IC_{50}), the FU-free nano-vehicle was more cytotoxic than the FU-loaded nano-vehicle.

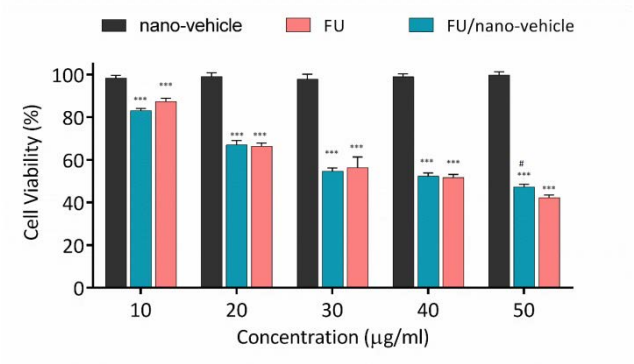

Figure 2. Cytotoxicity evaluation by MTT assay. The A549 cells treated with FU, FU/nano-vehicle, and blank nano-vehicle for 48 h. *** p<.001 versus nano-vehicle group. # p < 0.5versus FU group

Qualitative intracellular uptake by fluorescence microscopy

The cellular uptake and internalization of rhodamine-labeled nano-vehicle were evaluated in a time-dependent manner on A549 cancer cells, using fluorescence microscopy to evaluate the emission of rhodamine red fluorescence. Rhodamine generally helps track the uptake of nano-vehicles. The cells have a permeable membrane, and nano-sized materials can easily pass through several pathways (concentration gradients, active transport system, such as protein pumps and ion channels, and endocytosis).

Nanomaterials with a size of <100 nm need to be internalized by endocytosis in transport vesicles derived from the plasma membrane (45). As shown in Figure 3A-3B, cells treated with rhodamine-labeled nano-vehicle showed proper internalization after two and four hours. The cellular uptake of the free form of rhodamine was also evaluated as the control, and observations showed that the uptake of free rhodamine was higher than rhodamine-labeled nano-vehicle.

Quantitative intracellular uptake by flow cytometry

Since the uptake of nano-vehicle is enhanced by advancing time, as shown by fluorescence microscopy, quantitative flow cytometry was performed to determine the percentage of cellular uptake. The results revealed that the A549 cells treated with rhodamine-labeled nano-vehicle showed 4.03% uptake after two hours (Figure 4). The cells showed a higher uptake (8.75% uptake) after four hours. The difference in the cellular uptake of rhodamine-labeled nano-vehicle may be due to the individual labeling profile, membrane, cytoskeletal factors, and production of a different extracellular matrix (38).

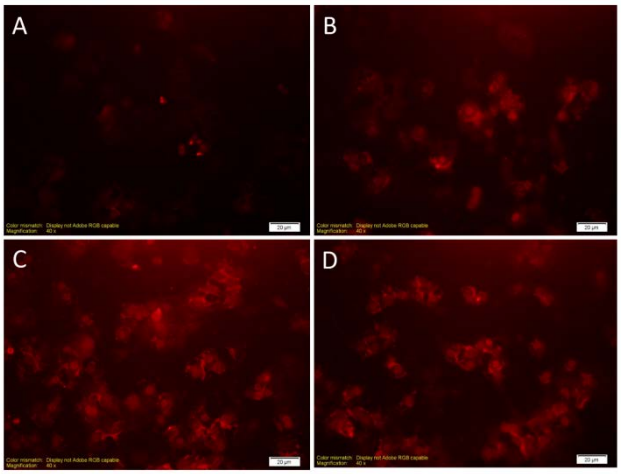

Figure 3. Cellular uptake evaluation of rhodamine-labeled nano-vehicle into the A549 cells after 2 (A) and 4 h (B) treatment by fluorescent microscopy. The cells treated with free rhodamine were also done for 2 (C) and 4 h (D) to consider as the controls

Apoptosis evaluation by DAPI staining

DAPI staining was selected as an assay to determine intact, apoptotic, and necrotic cells after treatment for 48 hours. As shown in Figure 5, the untreated cells and treated cells with the FU-free nano-vehicle showed no morphological changes. After treating the cells with the blank nano-vehicle, the population of cells was almost identical, while the cells treated with FU-free and FU-loaded nano-vehicles showed nucleus morphology changes with a decrease in cell population.

Apoptosis study by flow cytometry

After treatment of A549 cells with the blank nano-vehicle, FU-loaded nano-vehicle, and FU-free nano-vehicle for 48 hours, the cells were stained with annexin V and PI for evaluating the apoptosis rate. As shown in Figure 6, the graphs were divided into four gates, including gate 1, gate

2, gate 3, and gate 4, corresponding to healthy, early apoptosis, late apoptosis, and necrosis cells. The cells treated with the blank nano-vehicle showed good cell viability (75.81% healthy cells). This low viability might be attributed to the sedimentation of the nano-vehicle on cells, causing hypoxia (deficiency of oxygen reaching the tissues). Also, the apoptotic effects of the FU-free nano-vehicle and FU-loaded nano-vehicle were evaluated and compared. The results showed a higher rate of apoptosis in the A549 cells for the FU-free nano-vehicle due to the possibly low level of nano-vehicle uptake by the cells, as shown by the cellular uptake assays. For a better comparison, all flow cytometry data are summarized in Table 1.

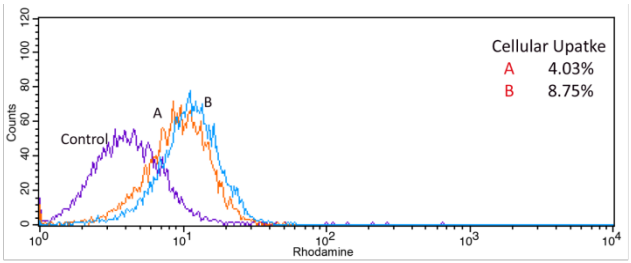

Figure 4. Cellular uptake evaluation of rhodamine-labeled nano-vehicle into the A549 cells after 2 (A) and 4 h (B) treatment by flow cytometry. The cells with no treatment consider as a negative control.

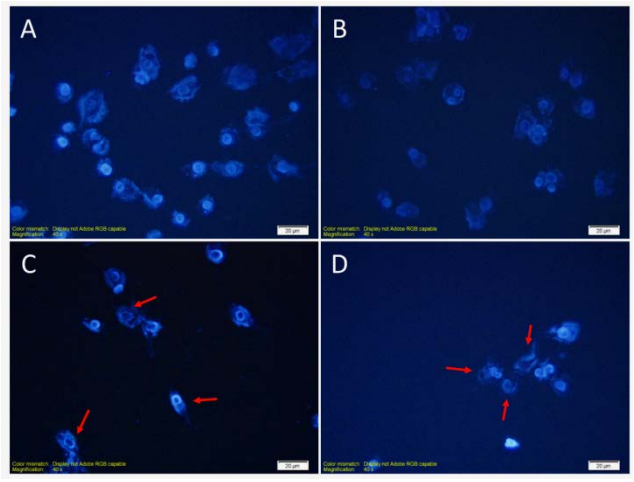

Figure 5. Apoptosis evaluation of nano-vehicle (B), free FU (C), and FU/nano-vehicle (D) on A549 cells after treatment for 48 h via fluorescent microscopy. The cells with no treatment consider as a control (A).

Table 1. Apoptosis analysis data for untreated (control) and treated cells after 48h

Sample	Gate 1	Gate 2	Gate 3	Gate 4
Control	99.92%	0.01%	0.00%	0.07%
Nano-vehicle	75.81%	14.88%	5.76%	3.55%
FU/nano-vehicle	35.10%	51.36%	13.32%	0.22%
Free FU	27.32%	41.16%	30.97%	0.55%

Gate 1 (healthy cells) - Gate 2 (early apoptosis) - Gate 3 (late apoptosis) - Gate 4 (necrosis)

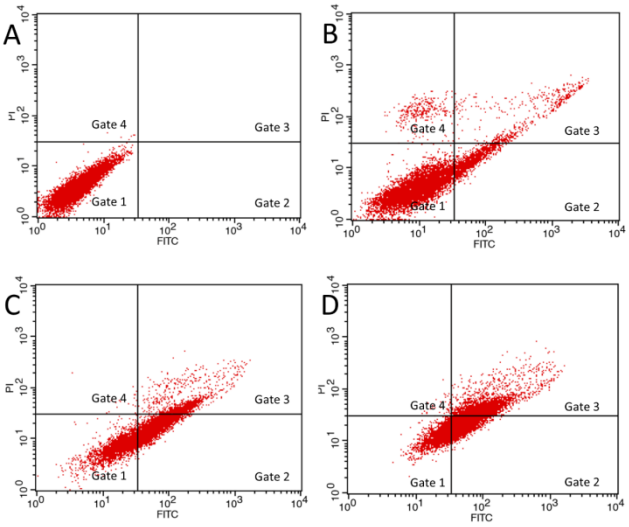

Figure 6. Apoptosis study of untreated (A) and treated samples including nano-vehicle (B), FU/nano-vehicle (C), and free FU (D) by flow-cytometry after treatment for 48 h

DISCUSSION

To improve the cytotoxic effects of FU as an anticancer agent on A549 cells, a drug nano-formulation was designed and prepared. The hybrid of Lys/PNIPAM-PVP/GO was used as a nano-vehicle for the delivery of FU to the A549 cancer cells. Cytotoxicity evaluation by MTT assay showed that the slightly low cytotoxicity of FU-loaded nano-vehicle, as compared to the FU-free nano-vehicle, was attributed to the sustained release of FU from the developed platform. On the other hand, the low rate of drug carrier internalization into the A549 cells may play a crucial role in the drug carrier efficacy. The qualitative cellular uptake by fluorescence microscopy showed that the uptake of free rhodamine was higher than rhodamine labeled nano-vehicle. The high rate of rhodamine uptake

by the cells can be justified by its smaller size compared to our designed nano-vehicle. The quantitative cellular uptake by flow cytometry showed that the low internalization of nano-vehicle into the A549 cells is the primary reason for the low toxicity of FU-loaded nano-vehicle on the A549 lung cancer cell line in comparison to the FU-free nano vehicle. Based on our recent study on the delivery of FU to cancer MCF7 cells by the same drug carrier, the MCF7 cells showed 100% uptake in the first two hours (38), since the FU/nano-vehicle had greater cytotoxic effects on the MCF7cells. The results revealed by DAPI staining showed that the FU-loaded nano-vehicle had higher apoptotic effects on the treated cells, in comparison to the chemotherapeutic FU agent. Apoptosis study by flow cytometry showed that the sustained release of FU from the nanocarrier also causes significantly low cytotoxic effects on the cells.

In conclusion, the most important properties of an ideal carrier include stability, nano-sized shape, high drug loading, biocompatibility, and lack of cytotoxic effects. A GO drug carrier was developed and used in this study on the A549 human lung cancer cells. The biocompatibility of the nano-vehicle was confirmed by MTT assay, DAPI staining, and apoptosis assay. The results showed that the nano-vehicle had no substantial cytotoxic effects on the cells. Cellular uptake assays were also performed via both fluorescence microscopy and flow cytometry. Both analyses revealed the low internalization of the nano-vehicle into the A549 cancer cells, with 10% cellular uptake in the first four hours of treatment. The low penetration rate led to the low toxicity of drug-loaded nano-vehicle. To confirm the results, both DAPI and FITC-Annexin V staining were performed as apoptosis assays to show apoptosis and necrosis in the treated cells.

REFERENCES

1. Yarmohamadi A, Asadi J, Gharaei R, Mir M, Khoshnazar AK. Valproic acid, a histone deacetylase inhibitor, enhances radiosensitivity in breast cancer cell line. ***Journal of Radiation and Cancer Research*** 2018;9(2):86.
2. Global Burden of Disease Cancer Collaboration, Fitzmaurice C, Abate D, Abbasi N, Abbastabar H, Abd-Allah F, et al. Global, Regional, and National Cancer Incidence, Mortality, Years of Life Lost, Years Lived With Disability, and Disability-Adjusted Life-Years for 29 Cancer Groups, 1990 to 2017: A Systematic Analysis for the Global Burden of Disease Study. ***JAMA Oncol*** 2019;5(12):1749-1768.
3. GBD 2017 Stomach Cancer Collaborators. The global, regional, and national burden of stomach cancer in 195 countries, 1990-2017: a systematic analysis for the Global Burden of Disease study 2017. ***Lancet Gastroenterol Hepatol*** 2020;5(1):42-54.
4. GBD 2017 Pancreatic Cancer Collaborators. The global, regional, and national burden of pancreatic cancer and its attributable risk factors in 195 countries and territories, 1990-2017: a systematic analysis for the Global Burden of Disease Study 2017. ***Lancet Gastroenterol Hepatol*** 2019;4(12):934-947.
5. Bray F, Ferlay J, Soerjomataram I, Siegel RL, Torre LA, Jemal A. Global cancer statistics 2018: GLOBOCAN estimates of incidence and mortality worldwide for 36 cancers in 185 countries. ***CA Cancer J Clin*** 2018;68(6):394-424.
6. Siegel RL, Miller KD, Jemal A. Cancer statistics, 2018. ***CA Cancer J Clin*** 2018;68(1):7-30.
7. Rahimi M, Shojaei S, Safa KD, Ghasemi Z, Salehi R, Yousefi B, et al. Biocompatible magnetic tris (2-aminoethyl) amine functionalized nanocrystalline cellulose as a novel nanocarrier for anticancer drug delivery of methotrexate. ***New Journal of Chemistry*** 2017;41(5):2160-8.
8. Lv PP, Ma YF, Yu R, Yue H, Ni DZ, Wei W, et al. Targeted delivery of insoluble cargo (paclitaxel) by PEGylated chitosan nanoparticles grafted with Arg-Gly-Asp (RGD). ***Mol Pharm*** 2012;9(6):1736-47.
9. Zhang R, Fan Q, Yang M, Cheng K, Lu X, Zhang L, et al. Engineering Melanin Nanoparticles as an Efficient Drug-Delivery System for Imaging-Guided Chemotherapy. ***Adv Mater*** 2015;27(34):5063-9.
10. Wang YX, Guo DS, Duan YC, Wang YJ, Liu Y. Amphiphilic p-sulfonatocalix[4]arene as "drug chaperone" for escorting anticancer drugs. ***Sci Rep*** 2015;5:9019.
11. Rahimi M, Safa KD, Salehi R. Co-delivery of doxorubicin and methotrexate by dendritic chitosan-g-mPEG as a magnetic

nanocarrier for multi-drug delivery in combination chemotherapy. ***Polymer Chemistry*** 2017;8(47):7333-50.

12. Shafiei-Irannejad V, Samadi N, Salehi R, Yousefi B, Rahimi M, Akbarzadeh A, et al. Reversion of Multidrug Resistance by Co-Encapsulation of Doxorubicin and Metformin in Poly(lactide-co-glycolide)-d-α-tocopheryl Polyethylene Glycol 1000 Succinate Nanoparticles. ***Pharm Res*** 2018;35(6):119.
13. Ahmadkhani L, Akbarzadeh A, Abbasian M. Development and characterization dual responsive magnetic nanocomposites for targeted drug delivery systems. ***Artif Cells Nanomed Biotechnol*** 2018;46(5):1052-1063.
14. Salehi R, Davaran S, Rashidi MR, Entezami AA. Thermosensitive nanoparticles prepared from poly (N-isopropylacrylamide-acrylamide-vinilpyrrolidone) and its blend with poly (lactide-co-glycolide) for efficient drug delivery system. ***Journal of applied polymer science*** 2009;111(4):1905-10.
15. Rahimi M, Karimian R, Mostafidi E, Noruzi EB, Taghizadeh S, Shokouhi B, et al. Highly branched amine-functionalized p-sulfonatocalix [4] arene decorated with human plasma proteins as a smart, targeted, and stealthy nano-vehicle for the combination chemotherapy of MCF7 cells. ***New Journal of Chemistry*** 2018;42(15):13010-24.
16. Karimian A, Parsian H, Majidinia M, Rahimi M, Mir SM, Samadi Kafil H, et al. Nanocrystalline cellulose: Preparation, physicochemical properties, and applications in drug delivery systems. ***Int J Biol Macromol*** 2019;133:850-859.
17. Majidinia M, Mirza-Aghazadeh-Attari M, Rahimi M, Mihanfar A, Karimian A, Safa A, et al. Overcoming multidrug resistance in cancer: Recent progress in nanotechnology and new horizons. ***IUBMB Life*** 2020;72(5):855-871.
18. Franzé S, Marengo A, Stella B, Minghetti P, Arpicco S, Cilurzo F. Hyaluronan-decorated liposomes as drug delivery systems for cutaneous administration. ***Int J Pharm*** 2018;535(1-2):333-339.
19. Kosakowska KA, Casey BK, Kurtz SL, Lawson LB, Grayson SM. Evaluation of Amphiphilic Star/Linear-Dendritic Polymer Reverse Micelles for Transdermal Drug Delivery: Directing Carrier Properties by Tailoring Core versus Peripheral Branching. ***Biomacromolecules*** 2018;19(8):3163-3176.
20. Salehi R, Hamishehkar H, Eskandani M, Mahkam M, Davaran S. Development of dual responsive nanocomposite for simultaneous delivery of anticancer drugs. ***J Drug Target*** 2014;22(4):327-42.
21. Rahimi M, Shafiei-Irannejad V, D Safa K, Salehi R. Multi-branched ionic liquid-chitosan as a smart and biocompatible nano-vehicle for combination chemotherapy with stealth and targeted properties. ***Carbohydr Polym*** 2018;196:299-312.
22. Kim DH, Lu N, Ghaffari R, Kim YS, Lee SP, Xu L, et al. Materials for multifunctional balloon catheters with capabilities in cardiac electrophysiological mapping and ablation therapy. ***Nat Mater*** 2011;10(4):316-23.
23. Rakhshaei R, Namazi H, Hamishehkar H, Rahimi M. Graphene quantum dot cross-linked carboxymethyl cellulose nanocomposite hydrogel for pH-sensitive oral anticancer drug delivery with potential bioimaging properties. ***Int J Biol Macromol*** 2020;150:1121-1129.
24. Ahmadi D, Zarei M, Rahimi M, Khazaie M, Asemi Z, Mir SM, et al. Preparation and in-vitro evaluation of pH-responsive cationic cyclodextrin coated magnetic nanoparticles for delivery of methotrexate to the Saos-2 bone cancer cells. ***Journal of Drug Delivery Science and Technology*** 2020;57:101584.
25. Liu J, Cui L, Losic D. Graphene and graphene oxide as new nanocarriers for drug delivery applications. ***Acta Biomater*** 2013;9(12):9243-57.
26. McCallion C, Burthem J, Rees-Unwin K, Golovanov A, Pluen A. Graphene in therapeutics delivery: Problems, solutions and future opportunities. ***Eur J Pharm Biopharm*** 2016;104:235-50.
27. Jafarirad S, Hammami Torghabe E, Rasta SH, Salehi R. A novel non-invasive strategy for low-level laser-induced cancer therapy by using new Ag/ZnO and Nd/ZnO functionalized reduced graphene oxide nanocomposites. ***Artif Cells Nanomed Biotechnol*** 2018;46(sup2):800-816.
28. Song J, Gao H, Zhu G, Cao X, Shi X, Wang Y. The preparation and characterization of polycaprolactone/graphene oxide biocomposite nanofiber scaffolds and their application for directing cell behaviors. ***Carbon*** 2015;95:1039-50.

29. Yadav M, Rhee KY, Park SJ. Synthesis and characterization of graphene oxide/carboxymethylcellulose/alginate composite blend films. ***Carbohydr Polym*** 2014;110:18-25.
30. Torchilin VP. Multifunctional, stimuli-sensitive nanoparticulate systems for drug delivery. ***Nat Rev Drug Discov*** 2014;13(11):813-27.
31. Zhao Y, Zhou Y, Wang D, Gao Y, Li J, Ma S, et al. pH-responsive polymeric micelles based on poly(2-ethyl-2-oxazoline)-poly(D,L-lactide) for tumor-targeting and controlled delivery of doxorubicin and P-glycoprotein inhibitor. ***Acta Biomater*** 2015;17:182-92.
32. Deb A, R V. Natural and synthetic polymer for graphene oxide mediated anticancer drug delivery-A comparative study. Int J Biol Macromol. 2018 Feb;107(Pt B):2320-2333.
33. Sung B, Kim C, Kim MH. Biodegradable colloidal microgels with tunable thermosensitive volume phase transitions for controllable drug delivery. ***J Colloid Interface Sci*** 2015;450:26-33.
34. Amani H, Mostafavi E, Arzaghi H, Davaran S, Akbarzadeh A, Akhavan O, et al. Three-Dimensional Graphene Foams: Synthesis, Properties, Biocompatibility, Biodegradability, and Applications in Tissue Engineering. ***ACS Biomater Sci Eng*** 2019;5(1):193-214.
35. Kazempour M, Namazi H, Akbarzadeh A, Kabiri R. Synthesis and characterization of PEG-functionalized graphene oxide as an effective pH-sensitive drug carrier. ***Artif Cells Nanomed Biotechnol*** 2019;47(1):90-94.
36. Kazempour M, Edjlali L, Akbarzadeh A, Davaran S, Farid SS. Synthesis and characterization of dual pH-and thermo-responsive graphene-based nanocarrier for effective anticancer drug delivery. ***Journal of Drug Delivery Science and Technology*** 2019;54:101158.
37. Rao Z, Ge H, Liu L, Zhu C, Min L, Liu M, et al. Carboxymethyl cellulose modified graphene oxide as pH-sensitive drug delivery system. ***Int J Biol Macromol*** 2018;107(Pt A):1184-1192.
38. Ashjaran M, Babazadeh M, Akbarzadeh A, Davaran S, Salehi R. Stimuli-responsive polyvinylpyrrolidone-NIPPAm-lysine graphene oxide nano-hybrid as an anticancer drug delivery on MCF7 cell line. ***Artif Cells Nanomed Biotechnol*** 2019;47(1):443-454.
39. Guo HL, Wang XF, Qian QY, Wang FB, Xia XH. A green approach to the synthesis of graphene nanosheets. ***ACS Nano*** 2009;3(9):2653-9.
40. Farshbaf M, Salehi R, Annabi N, Khalilov R, Akbarzadeh A, Davaran S. pH- and thermo-sensitive MTX-loaded magnetic nanocomposites: synthesis, characterization, and in vitro studies on A549 lung cancer cell and MR imaging. ***Drug Dev Ind Pharm*** 2018;44(3):452-462.
41. Farshbaf M, Salehi R, Annabi N, Khalilov R, Akbarzadeh A, Davaran S. pH- and thermo-sensitive MTX-loaded magnetic nanocomposites: synthesis, characterization, and in vitro studies on A549 lung cancer cell and MR imaging. ***Drug Dev Ind Pharm*** 2018;44(3):452-462.
42. Shafiei-Irannejad V, Rahimi M, Zarei M, Dinparast-Isaleh R, Bahrambeigi S, Alihemmati A, et al. Polyelectrolyte Carboxymethyl Cellulose for Enhanced Delivery of Doxorubicin in MCF7 Breast Cancer Cells: Toxicological Evaluations in Mice Model. ***Pharm Res*** 2019;36(5):68.
43. Venugopal K, Rather HA, Rajagopal K, Shanthi MP, Sheriff K, Illiyas M, et al. Synthesis of silver nanoparticles (Ag NPs) for anticancer activities (MCF 7 breast and A549 lung cell lines) of the crude extract of Syzygium aromaticum. ***J Photochem Photobiol B*** 2017;167:282-289.
44. Wang T, Hou J, Su C, Zhao L, Shi Y. Hyaluronic acid-coated chitosan nanoparticles induce ROS-mediated tumor cell apoptosis and enhance antitumor efficiency by targeted drug delivery via CD44. ***J Nanobiotechnology*** 2017;15(1):7.
45. Rahimi M, Karimian R, Noruzi EB, Ganbarov K, Zarei M, Kamounah FS, et al. Needle-shaped amphoteric calix[4]arene as a magnetic nanocarrier for simultaneous delivery of anticancer drugs to the breast cancer cells. ***Int J Nanomedicine*** 2019;14:2619-2636.